Analytical Performance of Inductively Coupled Plasma Emission Spectrometry Using Argon–Nitrogen Binary and Argon–Helium–Nitrogen Ternary Gas Mixture System

Kazuaki WAGATSUMA and Kichinosuke HIROKAWA

Institute for Materials Research, Tohoku University, Katahira, Sendai 980, Japan

Analytical performance of mixed gas inductively coupled plasmas (ICP) of argon–nitrogen binary and argon–helium–nitrogen ternary system was investigated for seven elements (Mg, Ca, Ba, Zn, Cd, Fe, and Y) having different ionization potentials, to yield the following. (1) In argon–nitrogen mixed gas ICPs, one should select higher flow rates of the carrier gas than in the argon ICP to obtain the appropriate signal-to-background ratio (SBR). (2) The ternary mixed gas plasmas yield better operating conditions regarding the SBR, because helium suppresses any increase in the background level caused by the nitrogen addition.

Keywords Inductively coupled plasma, argon–nitrogen mixed gas, argon–nitrogen–helium mixed gas, group-II elements, signal-to-background ratio

Several researchers have suggested it as an advantageous modification of the inductively coupled plasma (ICP) to replace part or all of the argon gas with other gases.[1-13] In most cases, an argon–nitrogen mixture system became an object of research because running cost for operating the ICP could be reduced by using nitrogen gas. Spectroscopic analyses have revealed the features of the argon–nitrogen ICP in comparison to those of the pure argon ICP. Montaser *et al.* reported the effect of nitrogen gas in the outer gas flow on the emission intensities of the analytes and provided some interesting results on the analytical performance of an argon–nitrogen ICP.[7,8] The performance of an argon-matrix plasma containing *ca.* 5% nitrogen gas was superior to that of the pure argon plasma; the optimum observation height was reduced, compared to the conditions obtained with argon gas alone. Spectroscopic features of an argon–nitrogen ICP were investigated by Choot *et al.* Their results indicated that the emission intensities from singly-ionized atoms were uniquely enhanced relative to those of neutral atoms when nitrogen was added to the plasma.[9-11] Their studies suggested that the mixed gas plasma yields different excitation and ionization conditions when compared with the argon plasma.[10] Choot *et al.* also studied an argon–helium mixed gas ICP[10], and found that the background continuum in the argon–helium ICP is rather low compared to the pure argon ICP. The decrease in the background intensity results in an increase in the signal-to-noise ratio by a factor of 2 – 3 over that of the pure argon plasma.[10]

In this paper, we investigated the analytical performance of an ICP supported by argon–helium gas mixtures containing a small amount of nitrogen. The fluctuation of the emission signals is closely dependent on the magnitude of the background. In general, higher background levels worsen the deviation of the spectral intensities detected, and thus the precision of the analytical results declines. It should be noted that the helium addition is able to suppress the background levels. The effect offers an advantage over the pure argon ICP, particularly when the ICP is operated under the high power conditions. On the other hand, the nitrogen addition to the argon ICP causes an increase in the background heights as well as the spectral intensities.[8,10,13] Accordingly, it is worthwhile to investigate the mixed gas ICP using an argon–helium–nitrogen ternary gas system for improving the analytical performance. The effects of the helium addition on the line and background intensities are discussed in comparison to those of the argon–nitrogen binary gas mixtures.

Some elements belonging to the group II in the periodic table: magnesium, calcium, barium, cadmium, and zinc, were selected as the test samples. They have similar electronic configurations[14], although their ionization potentials are different. For each element, one can employ analytical lines which are identified to the analogous transition schemes. These emission lines can be available for investigating the effect of the ionization potential on excitation and ionization mechanisms in the ICP. In addition, iron and yttrium were also studied. The former is the most common element for industrial materials and the latter is frequently employed as the internal standard in the ICP analysis.

Table 1 Instrumentation (a) and experimental conditions (b)

(a)	
Plasma source unit	ICPS-2H model (Shimadzu Corp., Japan)
R.f. generator	frequency: 27.12 MHz, 2.7 kW max
Induction coil	two turns, 30 mm i.d.
Torch	Fassel-type, outer gas tube of 18 mm i.d.
Nebulizer	Pneumatic
Spray chamber	Scott-type double pass
Spectrometer	GE-340 model (Shimadzu Corp., Japan)
	focal length: 3.4 m; grating: 1200 grooves/mm; blaze wavelength: 300 nm; slit: 30 μm width, 3 mm height
Photomultiplier	R-955 (Hamamatsu Photonics Corp., Japan)
Optics	fused-silica lens, focusing a 1 : 1 image of the plasma source on the entrance slit
Gas mixer	MX-3S model (Yutaka Eng. Corp., Japan)
(b)	
Incident r.f. power	1.6 kW
Reflected power	less than 40 W, see text
Outer gas flow rate	Ar + He 16.0 l/min (fixed) and N_2 0 – 0.6 l/min (as parameter),
	He composition in Ar–He mixture: 0, 6.3, 9.4, 12.5, 15.6 or 18.8%
Intermediate gas rate	Ar 1.4 l/min (fixed)
Carrier gas rate	Ar 1.0, 1.2, or 1.4 l/min (as parameter)
Observation height	14 mm above load coil (fixed)
Sample uptake rate	*ca.* 1.6 ml/min when distilled water is injected

Experimental

Apparatus

Our plasma source unit consisted of a plasma torch, a matching box, and a radio frequency generator. No modification of the unit was carried out. A Fastie–Ebert mounting spectrograph, equipped with a photomultiplier tube, was employed. The emission intensities were recorded while scanning the wavelengths on an analog pen recorder. Table 1 describes all other instrumentation and the operating conditions in detail.

Reagents

Stock solutions of cadmium, zinc, and iron were prepared by dissolving each high purity metal (more pure than 99.999% in zinc and iron, 99.9% pure in cadmium) in small amounts of heated hydrochloric acid (6 M) in zinc and iron or heated nitric acid (7 M) in cadmium, and by subsequent dilution to a concentration of 10 mg/ml with distilled water. Test solutions of the zinc and the iron concentration of 0.01 mg/ml were made by diluting with appropriate amounts of dilute hydrochloric acid. A test solution of the cadmium concentration of 0.01 mg/ml was also made by diluting with appropriate amounts of dilute nitric acid. All the solutions contained *ca.* 0.04 M hydrochloric or nitric acid.

Stock solutions of magnesium, calcium, barium, and yttrium were prepared by dissolving each metal carbonate of 99.9% purity (oxide in yttrium, 99.9% pure) in small amounts of hydrochloric acid (6 M) by gentle heating, and by subsequent dilution to a concentration of 10 mg/ml with distilled water. The metal concentration in test solutions was 0.0005 mg/ml for magnesium, 0.001 mg/ml for calcium, and 0.005 mg/ml for barium and yttrium, respectively. All the solutions contained less than 0.01 M hydrochloric acid.

Analytical lines

For each of the elements, one or a few analytical emission lines were selected as listed in Table 2. These lines are assigned to resonance transitions of the singly-ionized species. The Cd I 228.80 nm line was measured only for the estimation of the ion-to-atom line ratio. Because both the atomic and the ionic lines exhibit similar excitation energies[14], the relative population of the ionic species to the neutrals can be deduced from the ion-to-atom line ratios. Signal-to-background ratios were calculated from measurement of the background intensity at an adjacent wavelength for each analytical line.

Procedure

Mixed gases were introduced only as the outer gas flow of the ICP. For the intermediate and the carrier gas flow, pure argon was employed at the fixed flow rates. The argon–helium mixed gases having six different compositions: 0, 6.3, 9.4, 12.5, 15.6, or 18.8% He, were examined. The total flow rate of the mixtures was kept at 16.0 l/min and then relatively small amounts of nitrogen were added to the outer gas flow. The nitrogen rate was varied from 0 to 0.6 l/min. Because the matching networks in our instrumentation were designed for pure argon, it was difficult to control the reflected power appropriately at higher nitrogen flow rates. The resultant discharge became unstable and extinguished when the reflected power exceeded more than *ca.* 40 W. Therefore, the upper limit of the nitrogen content was restricted by the instrumental ability to adjust the reflected power. The allowed content of nitrogen was lowered when the gas flow contained higher contents of helium gas. The plasma was initiated with argon gas only. Once the stable discharge was obtained, an appropriate amount of argon was gradually replaced

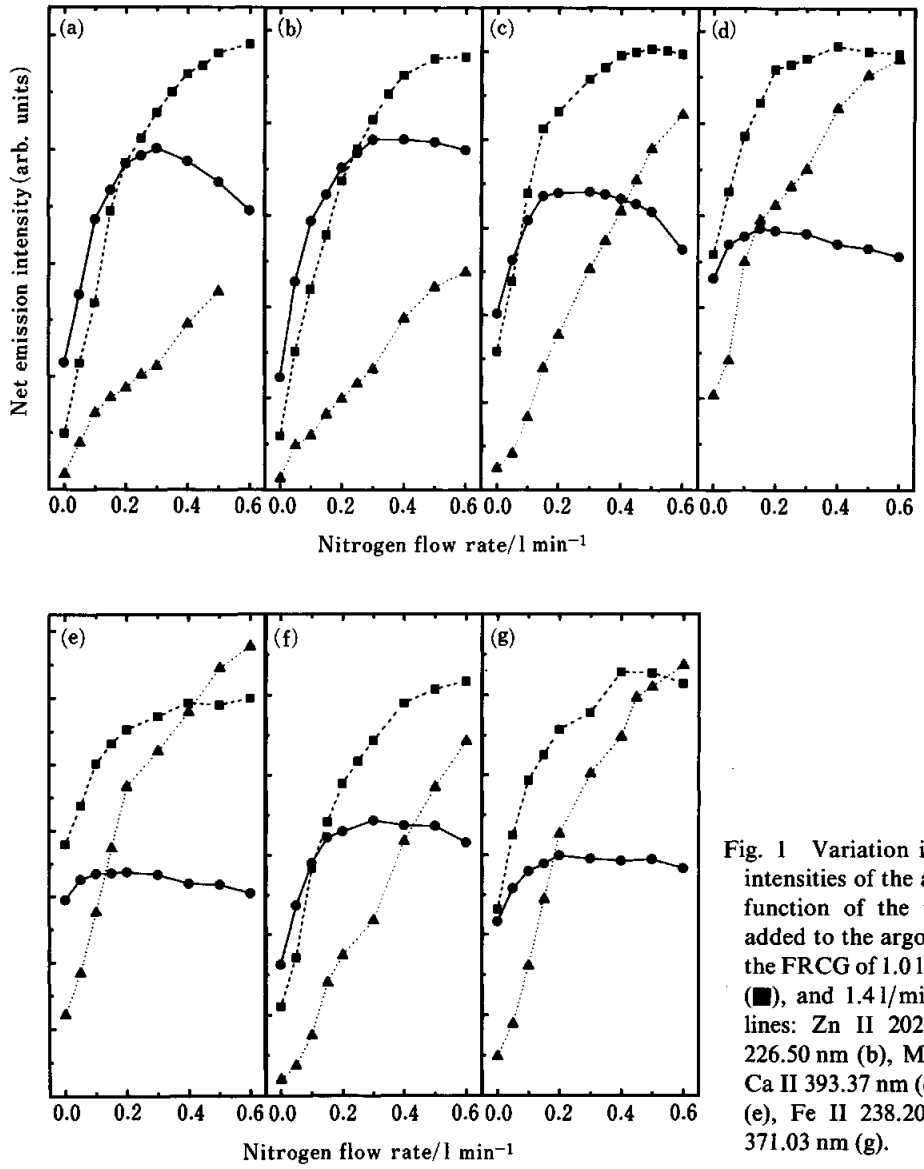

Fig. 1 Variation in the net emission intensities of the analytical lines as a function of the nitrogen flow rate added to the argon outer gas flow at the FRCG of 1.0 l/min (●), 1.2 l/min (■), and 1.4 l/min (▲). Analytical lines: Zn II 202.55 nm (a), Cd II 226.50 nm (b), Mg II 279.55 nm (c), Ca II 393.37 nm (d), Ba II 455.40 nm (e), Fe II 238.20 nm (f), and Y II 371.03 nm (g).

with helium gas while any variations in the reflected power were checked.

The emission intensities of the analytical lines were estimated from the average peak height for three or four replicates. The results exhibited good precision and the relative standard deviations were within a few %.

Results and Discussion

Argon–nitrogen binary gas mixture ICP

Figure 1 indicates variations in the emission intensities of the analytical lines as a function of the nitrogen flow rate added for different flow rates of the carrier gas (FRCG). The carrier gas flow is a very critical parameter in the ICP emission spectrometry. Changes in the spectral intensities with the FRCG are derived from the change in both the sampling rate of aerosol and the characteristics of the plasma itself.[15] In the conventional argon ICP spectrometry, the optimum conditions are obtained at relatively low FRCGs, indicating that a change in the excitation efficiency caused by the increase in the flow rate is a more dominant factor for determination of the analytical conditions compared to that in injection amounts of the sample solution. In our instrument, the FRCG of 1.0 l/min was recommended by the manufacturer. It is interesting to investigate the optimum conditions regarding the FRCG when nitrogen gas is added to the pure argon plasma.

As shown in Figs. 1a (Zn II 202.55 nm) and 1b (Cd II 226.50 nm), the greatest intensities of these emission lines are obtained at the FRCG of 1.0 l/min when pure argon is employed (the rate of nitrogen gas is zero). It can be found that the emission intensities are raised in all the cases of the FRCG with increasing the nitrogen flow rate added. Whereas the cadmium intensities reach steady states at the FRCG of 1.0 or 1.2 l/min, those at 1.4 l/min monotonously increase with an increase in the nitrogen rate. Especially, when the flow rate of nitrogen gas

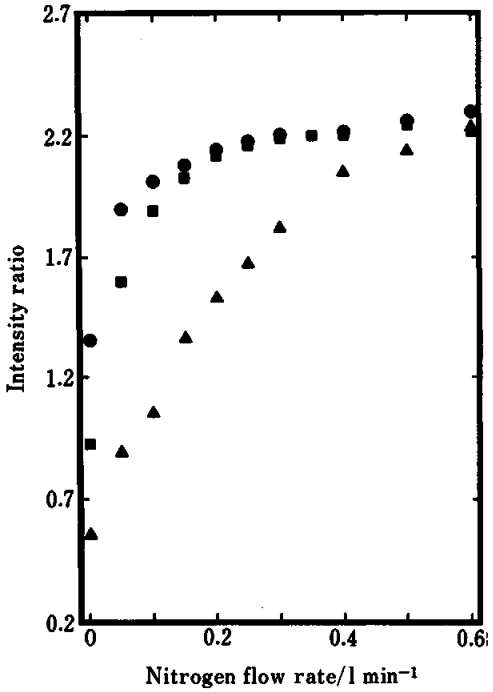

Fig. 2 Change in the intensity ratio (Cd II 226.50/Cd I 228.80) as a function of the nitrogen flow rate added at the FRCGs: 1.0 l/min (●), 1.2 l/min (■), and 1.4 l/min (▲).

exceeds *ca.* 0.2 – 0.3 l/min in the argon–nitrogen mixed gas ICP, the emission intensities observed at the FRCG of 1.2 l/min (closed squares in Fig. 1) become greater than those at 1.0 l/min (closed circles in Fig. 1). However, the intensities obtained at the FRCG of 1.4 l/min are always smallest independent of the FRCG in the argon–nitrogen mixed gas ICP.

On the other hand, in the calcium (Ca II 393.37 nm) or the barium (Ba II 455.40 nm) lines, the desired emission intensities cannot be obtained when using the FRCG of 1.0 l/min (see Figs. 1d and 1e). Though the nitrogen addition causes an increase in the intensities of such emission lines, these variations observed at the FRCG of 1.0 l/min are very slight compared to those at 1.2 or 1.4 l/min. However, in the FRCG of 1.4 l/min (closed triangles), the emission intensities dominantly increase along with the flow rate of nitrogen gas added. In the case of the barium emission line, the intensities obtained at the FRCG of 1.4 l/min are greatest when the nitrogen rate is more than 0.4 l/min in the argon–nitrogen mixed gas ICP.

It has been reported that the addition of nitrogen can induce the elevation in the plasma temperature and thus exert a significant effect on the excitation and ionization of the analyte species in the plasma.[7,10,13] Furthermore, the plasma temperature varies also as a function of the flow rate of the carrier gas.[16] Generally, at the higher flow rates, the excitation and the ionization reactions in the plasma declined, principally due to the decrease in the plasma temperature. Figure 2 shows plots of the ion-to-atom line intensity ratio (Cd II 226.50/Cd I 228.80) as a function of the nitrogen flow rate for different FRCGs.

Table 2 Assignment of emission lines employed

Wavelength/ nm	Assignment Upper/eV	—	Lower/eV
Mg II 279.55	4.434, 3p $^2P_{3/2}$	—	0.000, 3s $^2S_{1/2}$
Ca II 393.37	3.151, 4p $^2P_{3/2}$	—	0.000, 4s $^2S_{1/2}$
Ba II 455.40	2.722, 6p $^2P_{3/2}$	—	0.000, 6s $^2S_{1/2}$
Zn II 202.55	6.119, 4p $^2P_{3/2}$	—	0.000, 4s $^2S_{1/2}$
Cd II 226.50	5.472, 5p $^2P_{1/2}$	—	0.000, 5s $^2S_{1/2}$
Cd I 228.80	5.417, 5s5p $^1P_1$	—	0.000, $(5s)^2$ $^1S_0$
Fe II 238.20	5.203, 4p $^6F_{11/2}$	—	0.000, 4s $^6D_{9/2}$
Y II 371.03	3.520, 5p $^3F_4$	—	0.180, 5s $^3D_3$

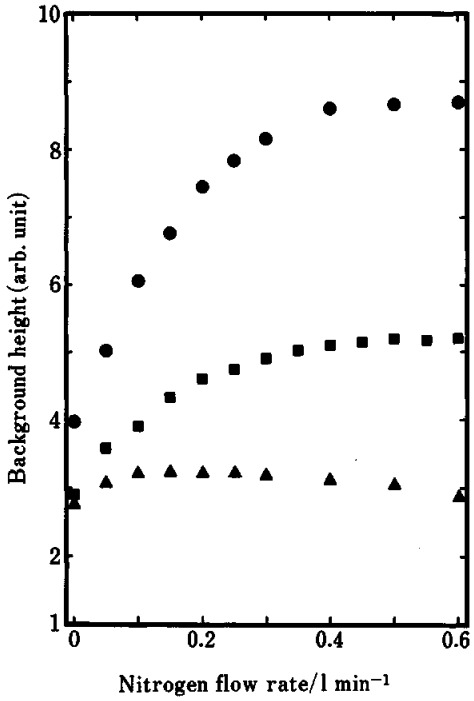

Fig. 3 Plots of the background height measured at 213.0 nm against the nitrogen flow rate for several carrier gas rates. The carrier gas rates employed are the same as in Fig. 1.

The ratio at the FRCG of 1.0 l/min is always larger than those measured at 1.2 l/min or 1.4 l/min. As denoted in Table 1, their excitation energies are approximately the same. We can deduce from these results that the ionization temperature becomes higher with increasing the flow rate of nitrogen gas added in all the cases of the FRCG. It was reported that the heat content of nitrogen gas is rather greater than that of argon.[17] Therefore, the heat capacity of the plasma may be enhanced by the nitrogen addition, because nitrogen molecules can act as an effective energy reservoir in the plasma, which leads to the more active excitation of the analyte species.

We find from Fig. 1 that variations in the emission intensities as a function of the FRCG strongly depend upon the kind of the spectral lines measured. We can

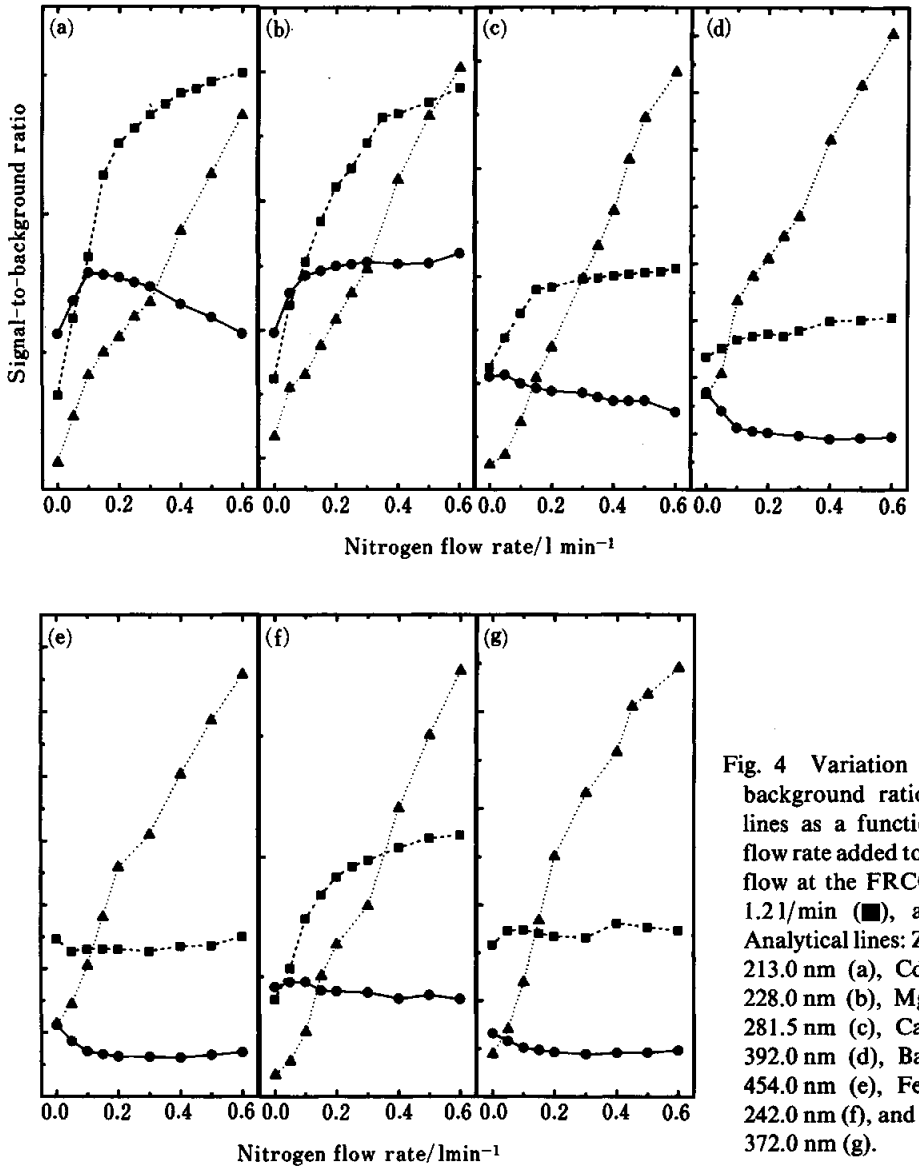

Fig. 4 Variation in the signal-to-background ratio of the analytical lines as a function of the nitrogen flow rate added to the argon outer gas flow at the FRCG of 1.0 l/min (●), 1.2 l/min (■), and 1.4 l/min (▲). Analytical lines: Zn II 202.55 nm/BG 213.0 nm (a), Cd II 226.50 nm/BG 228.0 nm (b), Mg II 279.55 nm/BG 281.5 nm (c), Ca II 393.37 nm/BG 392.0 nm (d), Ba II 455.40 nm/BG 454.0 nm (e), Fe II 238.20 nm/BG 242.0 nm (f), and Y II 371.03 nm/BG 372.0 nm (g).

consider that this result is principally due to the difference in the ionization potential between the sample elements. It should be noted that, in the elements having low ionization potentials, calcium (6.11 eV) and barium (5.20 eV)[14], the emission intensities are greater at higher flow rates of the carrier gas when nitrogen gas is added to the argon plasma. The emission intensity of a spectral line is determined by the population of the upper level of the corresponding transition. As indicated in Table 2, the analytical lines used in our work are identified with the transitions concerning excited states of the singly-ionized atoms. The relative population may be raised or reduced by redistribution among different ionized states and various excited states arising from changes in the plasma temperature. The ionization potential is an important parameter for determining the level distribution. As a result, behavior of the emission intensities in the mixed gas ICP is dependent on the kind of the sample element employed.

The behavior of the iron emission line for some FRCGs (Fig. 1f) is similar to that of the magnesium line (Fig. 1c). Further, the behavior of the yttrium emission line (Fig. 1g) is similar to that of the calcium line (Fig. 1d). These results may be explained from the similarity in the ionization potential between iron (7.90 eV) and magnesium (7.64 eV), yttrium (6.5 eV) and calcium (6.11 eV)[14], respectively.

Variations in the background height should be noted when argon–nitrogen gas mixtures are employed instead of pure argon. Figure 3 indicates changes in the background level measured at 213.0 nm as a function of the nitrogen flow rate. The background height is elevated as the amount of nitrogen increases. This result agrees with the previous report.[10] The background height at the FRCG of 1.2 l/min (closed squares in Fig. 3) are reduced by a factor of about 2 compared to that at 1.0 l/min (closed circles in Fig. 3). It is thus expected that, when the argon–nitrogen mixture system is used, the optimum conditions on the FRCG are different from those in the pure argon ICP.

We calculated the signal-to-background ratio (SBR) for each of the analytical emission lines in order to determine the optimum operating conditions in the argon–nitrogen mixed gas ICP. These results are illustrated in Fig. 4. In the elements whose ionization potentials are relatively low: calcium (Fig. 4d), barium (Fig. 4e), and yttrium (Fig. 4g), the SBRs decrease with an increase in the flow rate of nitrogen gas and then reach steady states when the FRCG is 1.0 l/min. On the other hand, when the FRCG is 1.4 l/min, the SBRs monotonously increase with increasing the amount of nitrogen in the plasma. The SBRs obtained at the 1.4 l/min FRCG are larger than those at the FRCG of 1.0 l/min by a factor of *ca.* 10 when the flow rate of nitrogen is 0.6 l/min in the mixed gas ICP. Therefore the FRCG of 1.4 l/min rather than 1.0 l/min should be selected for these elements. In zinc (Fig. 4a) and cadmium (Fig. 4b), the SBRs obtained at the 1.0 l/min FRCG are larger compared to those at the FRCGs of 1.2 l/min or 1.4 l/min when the flow rate of nitrogen gas is less than 0.1 l/min. However, as the content of nitrogen in the plasma is greater (more than *ca.* 0.2 l/min), the operation conditions using the FRCG of 1.2 l/min are superior to those using 1.0 l/min. The SBRs obtained at the 1.2 l/min FRCG are twice as great as those at 1.0 l/min, when the flow rate of nitrogen is 0.5 l/min.

The nitrogen addition in the argon ICP results in an increase in the background height of the emission spectrum measured. However, this disadvantage can be compensated by redetermining the amount of the carrier gas entering the plasma. Although the emission intensities also decrease at higher FRCG in the argon–nitrogen mixed gas ICP, the reduction in the background height caused by increasing the FRCG is more effective for determination of the optimum operation conditions.

Argon–helium–nitrogen ternary gas mixture ICP

In order to control the background height of the emission signal more appropriately, we examined the substitution of helium for argon in the outer gas flow using argon–nitrogen gas mixtures. Figure 5 shows a variation in the background level at 213.0 nm as a function of the helium content in the mixed gas ICP containing *ca.* 2.5% nitrogen for different FRCGs. It is found that the background heights are reduced with the content of helium in the ICP, as compared to the helium-free plasma.

The continuum background of the ICP results principally from radiative recombinations between argon ions and fast electrons.[18] Kinetic energies of the fast electrons are released as photons having a certain range of energies. The thermal conductivity of helium is about ten-times larger than that of argon.[17] Thus, much greater energies are able to be transferred through the elastic collisions between helium atoms and the electrons compared to in the collisions concerning argon species, indicating that the fast electrons are decelerated more effectively in the presence of helium. In the ICP containing helium, the reduction in the background level

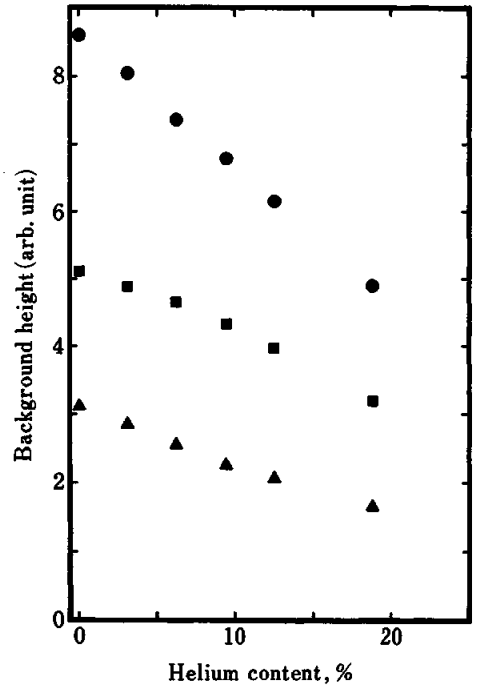

Fig. 5 Plots of the background height at 213.0 nm against the helium content in the outer gas flow comprising argon–helium–nitrogen ternary gas mixtures for several carrier gas flow rates. The carrier gas rates employed are the same as in Fig. 1.

may relate to changes in the energy distribution of free electrons in the plasma caused by the helium addition.[11]

Figure 6 shows variations of the SBR for each analytical emission line as a function of the helium content in the mixed gas ICP containing *ca.* 2.5% nitrogen. Whereas the SBRs obtained at the FRCG of 1.0 l/min stay constant independent of the helium content in the plasma, the SBRs at 1.4 l/min FRCG increase along with increasing the helium content. For all the elements investigated, the measurements using the FRCG of 1.4 l/min provide better SBR values compared to the results obtained at the other FRCGs. This effect in the argon–helium–nitrogen ICP is an significant advantage over the argon–nitrogen mixed gas ICP. It is interesting that the analytical performance in the argon–helium–nitrogen ICP closely depends not only on the composition of the plasma gas but also on the flow rate of the carrier gas.

References

1. D. Truitt and J. W. Robinson, *Anal. Chim. Acta,* **50**, 61 (1970).
2. D. Truitt and J. W. Robinson, *Anal. Chim. Acta,* **49**, 401 (1970).
3. K. Ohls and D. Sommer, *Fresenius' Z. Anal. Chem.,* **295**, 337 (1979).
4. L. Ebdon, M. R. Cave and D. J. Mowthrope, *Anal. Chim. Acta,* **115**, 171 (1980).
5. L. Ebdon, D. J. Mowthrope and M. R. Cave, *Anal. Chim.*

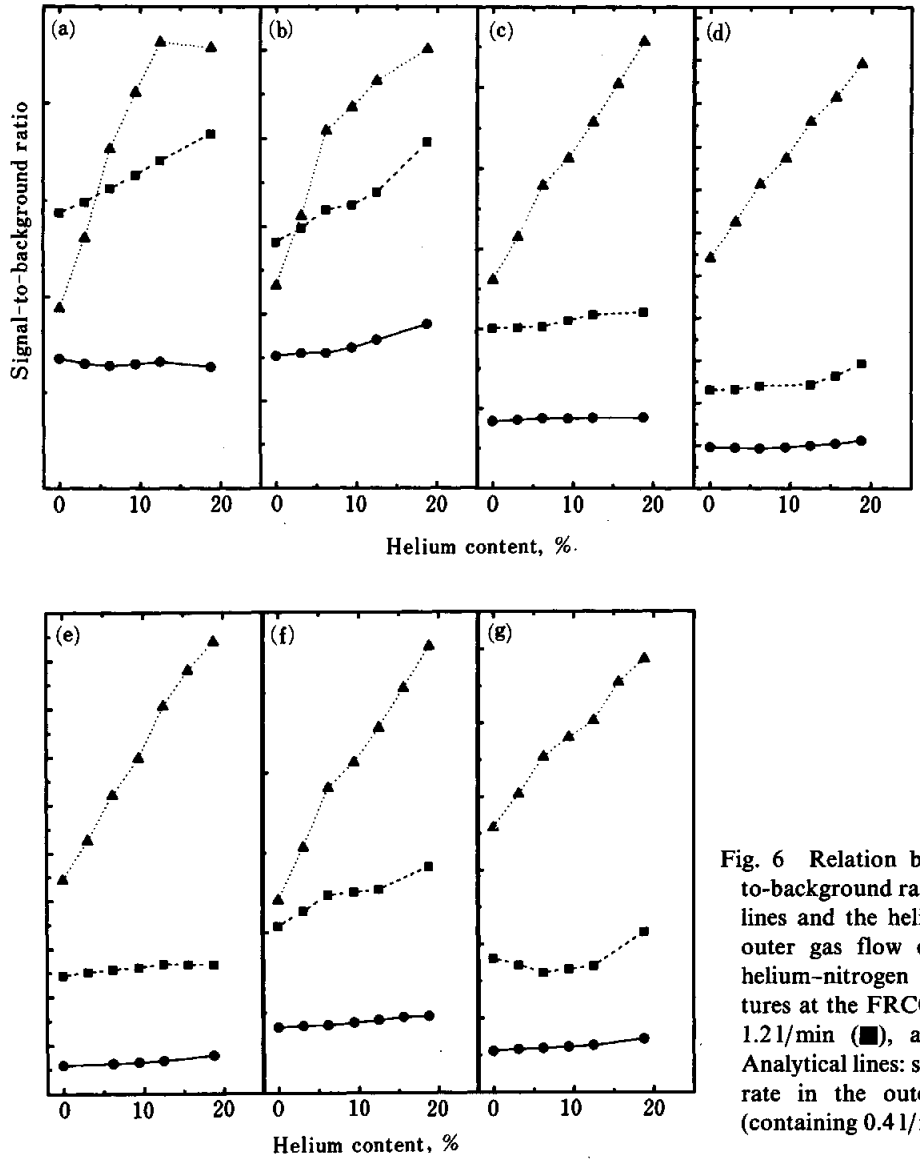

Fig. 6 Relation between the signal-to-background ratio of the analytical lines and the helium content in the outer gas flow comprising argon–helium–nitrogen ternary gas mixtures at the FRCG of 1.0 l/min (●), 1.2 l/min (■), and 1.4 l/min (▲). Analytical lines: see Fig. 4; total flow rate in the outer gas; 16.4 l/min (containing 0.4 l/min nitrogen).

Acta, **115**, 179 (1980).
6. S. Greenfield and D. T. Burns, *Anal. Chim. Acta,* **113**, 205 (1980).
7. A. Montaser and J. Mortazavi, *Anal. Chem.,* **52**, 225 (1980).
8. A. Montaser, V. A. Fassel and J. Zalewski, *Appl. Spectrosc.,* **35**, 292 (1981).
9. E. H. Choot and G. Horlick, *Spectrochim. Acta,* **41B**, 889 (1986).
10. E. H. Choot and G. Horlick, *Spectrochim. Acta,* **41B**, 925 (1986).
11. E. H. Choot and G. Horlick, *Spectrochim. Acta,* **41B**, 907 (1986).
12. K. Wagatsuma and K. Hirokawa, *Anal. Sci.,* **9**, 83 (1993).
13. K. Wagatsuma and K. Hirokawa, *Anal. Sci.,* **9**, 509 (1993).
14. C. E. Moore, "*Atomic Energy Levels*", NBS Circular 467, Vol. 1 (1949), Vol. 2 (1952), Vol. 3 (1961).
15. P. W. J. M. Boumans, "*Inductively Coupled Plasma Emission Spectroscopy*", ed. P. W. J. M. Boumans, Part I, Chap. 4, John Wiley & Sons, New York, (1987).
16. L. C. Bates and J. W. Olesik, *J. Anal. At. Spectrom.,* **5**, 239 (1990).
17. J. Hilsenrath, "*Tables of Thermal Properties of Gases*", NBS Circular, 564 (1955).
18. J. M. Mermet, "*Inductively Coupled Plasma Emission Spectroscopy*", ed. P. W. J. M. Boumans, Part II, Chap. 10, John Wiley & Sons, New York, 1987.

(Received December 27, 1993)
(Accepted March 1, 1994)